Passive Modeling of Transmission Line Impedance with Real Poles using Non-negative Least Squares

R. Mendoza-López, E.S. Bañuelos-Cabral, J.A. Gutiérrez-Robles, H.K. Høidalen and J.L. García-Sánchez.

***Abstract* – Rational function-based approximations are widely used to model frequency-dependent effects on power system components. In transmission line (TL) modeling, for example, series impedance behavior can be synthesized using these models for time-domain simulations. Due to its characteristics, the rational approximation of this impedance can be carried out with only real poles. Two rational fitting techniques are considered and compared, ensuring real poles: Vector Fitting-Real Poles (VF-RP) and Taku Noda's (TN) method. A fitting methodology based on residue calculation via Non-negative Least Squares (NNLS) is presented, which can be implemented in both fitters to obtain models that guarantee passivity. The advantages of the proposed methodology are demonstrated for (1) synthesizing the series impedance of a single-phase transmission line and (2) synthesizing the series impedance matrix of a three-phase double-circuit horizontal transmission line, where the concept of common poles is also implemented. The results show that the proposed methodology makes it possible to guarantee the passivity of the impedance model.**

***Keywords*: Model passivity, Non-negative Least Squares (NNLS), Rational approximation, Transmission line impedance modeling, Vector Fitting-Real Poles.**

I. Introduction

The frequency-dependent effects of power system components are synthesized and represented by rational function-based models obtained in the frequency domain through curve-fitting procedures [1-3]. These models are required to comply with a number of constraints associated with the behavior of physical systems: (1) stability, (2) realness, (3) reciprocity and (4) passivity. Constraints (1), (2) and (3) may be enforced by some existing rational fitting techniques and (4) is normally assessed and enforced by perturbation in a post-processing step [2, 4].

An important feature of the use of these models is that they can generally be associated with equivalent circuit representations [5]. Indeed, they have been used to represent an overhead transmission line (TL) directly in the time domain, incorporating the frequency dependence of the parameters caused by the skin effect and the ground-return effect [6-7]. Due to their nature, TL models can be synthesized using real poles only. It is possible to use rational fitting techniques that ensure rational approximation with real poles like Vector Fitting-Real Poles (VF-RP) [8] and Taku Noda's (TN) method [9].

R. Mendoza-López, E.S. Bañuelos-Cabral, J.A. Gutiérrez-Robles and J.L. García-Sánchez are with the University of Guadalajara, México.
H.K. Høidalen is with Norwegian University of Science and Technology, Norway.
(e-mail of corresponding author: eduardo.banuelos@academicos.udg.mx).
Paper submitted to the International Conference on Power Systems Transients (IPST2025) in Guadalajara, Mexico, June 8-12, 2025.

VF-RP is a methodology that slightly modifies the Vector Fitting (VF) procedure [10] to ensure a model with real poles and residues. It has been used to improve features of the Universal Line Model (ULM) [8] and the JMarti model [11], as well as for TL modeling in general [12-16]. The TN method was presented in [9] to synthesize a rational function-based model with real poles from tabulated frequency response data for TL impedance modeling. However, it could also be used to approximate smooth frequency responses with real poles. Both the VF-RP and TN methods deliver real poles and calculate the model's residues by using a single-step Least Squares (LS) method. The authors therefore propose applying the Non-negative Least Squares (NNLS) method, thus enabling passive cascade π-circuits that will take only energy from an external source.

This paper begins with an overview of the theoretical background for including the frequency-dependent effects of TL's modeling via cascaded π-circuits. Next, a description of the VF-RP and TN method is presented, followed by the implementation of NNLS to synthesize a model with positive parameters and thus guarantee its passivity. Then, the proposed methodology is demonstrated and the VF-RP and TN methods are compared in two test cases. Finally, the authors present their conclusions.

II. Cascade π-Circuits for Incorporating Frequency-Dependent Effects in TL Impedance Modeling.

As can be seen in Fig. 1, it is possible to use a cascade of π-circuits with N branches of RL-circuit in parallel to include the frequency dependence of the TL parameters [5-6]. These π-circuits are composed of resistors $R_0, R_1, \dots, R_N$ and inductors $L_0, L_1, \dots, L_N$ arranged in series of RL-branches. The transversal parameters are composed of a lumped capacitance C and conductance G. These parameters can be expressed as,

$$\begin{gathered} R_0 = R'_0\left(\frac{l}{m}\right), \quad R_1 = R'_1\left(\frac{l}{m}\right), \quad \dots \; R_N = R'_N\left(\frac{l}{m}\right). \\ L_0 = L'_0\left(\frac{l}{m}\right), \quad L_1 = L'_1\left(\frac{l}{m}\right), \quad \dots \; L_N = L'_N\left(\frac{l}{m}\right). \\ C = C'\left(\frac{l}{m}\right), \quad G = G'\left(\frac{l}{m}\right), \end{gathered} \tag{1}$$

with l being the length of the TL, m the number of π-circuits in cascade, and $R'_0, R'_1, \dots, R'_N, L'_0, L'_1, \dots, L'_N, C'$ and G' being the resistances, inductances, capacitance and conductance in per unit length (p.u.l.).

The calculated frequency-domain samples of the series impedance: $(s_k, \check{Z}_k)$ with $\check{Z}_k = \check{Z}(s_k)$ for $s_k = \mathrm{j}\omega_k$, $k = 1, \dots, K$ can be approximated as,

$$\check{Z}_k \cong Z(s;\mathbf{x}) = \sum_{n=1}^{N} \frac{sR'_n}{s + (R'_n/L'_n)} + R'_0 + sL'_0. \tag{2}$$

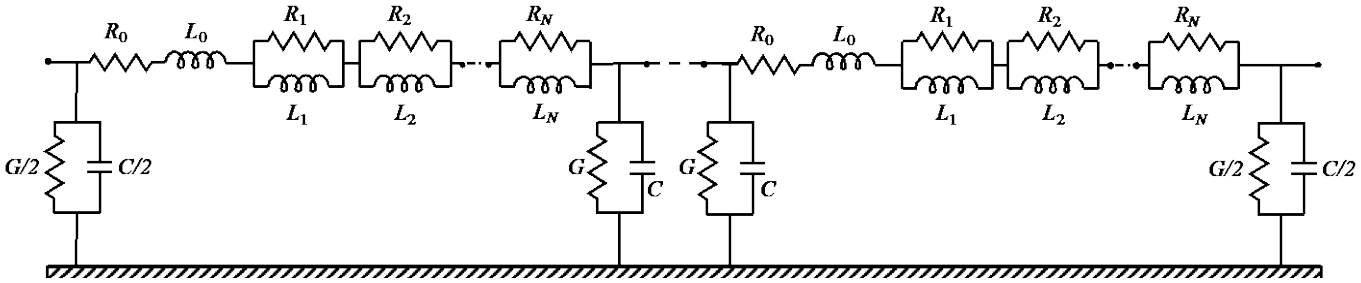

Fig. 1. Representation of a TL by a cascade of π-circuits with N branches of RL-circuit in parallel.

In (2), $\mathbf{x}$ represents a vector containing the model parameters for the rational approximation.

It is possible to conveniently modify (2) as,

$$\hat{Z}_k = \frac{\check{Z}_k - R'_0}{s} \cong \sum_{n=1}^{N} \frac{R'_n}{s + (R'_n/L'_n)} + L'_0. \tag{3}$$

With $R'_0 = R'_{dc}$. This formulation offers advantages during the fitting process that are discussed below.

$Z(s;\mathbf{x})$ in (2) comply with the necessary and sufficient conditions that a rational function must satisfy to be the impedance function of an RL circuit [17]:

1) $Z(s;\mathbf{x})$ is a positive real function.
2) $Z(s;\mathbf{x})$ has real poles on the negative real axis.
3) $Z(s;\mathbf{x})/s$ has positive real residues (3).
4) $Z(0)$ is either a positive constant or zero.

Both VF-RP and TN methods provide simple and stable poles, fulfilling almost the entire task. They do not, however, guarantee positive residues, which may result in some elements of the model being negative when they should be positive.

The constraint of positive residues will be incorporated by using Non-negative Least Squares (NNLS) and corroborated with the following relationship between poles (p_N) and zeros (z_N) of the rational approximation [17]:

$$0 \le p_1 < z_1 < p_2 < z_2 < \cdots p_N < z_N \le \infty. \tag{4}$$

III. Rational Approximation of Smooth Frequency-Domain Responses with Real Poles

This section briefly presents the methodology of Vector Fitting-Real Poles (VF-RP) [8] and Taku Noda's method [9], both proposed for obtaining rational approximations of smooth frequency-domain responses with real poles.

A. Vector Fitting-Real Poles (VF-RP)

The conventional VF process [10] calculates a rational function-based model from measured or calculated frequency-domain samples: $(s_k, \check{h}_k)$ with $\check{h}_k = \check{h}(s_k)$ for $s_k = \mathrm{j}\omega_k$, $k = 1, \ldots, K$.

$$\check{h}_k \cong h(s;\mathbf{x}) = \sum_{n=1}^{N} \frac{r_n}{s - p_n} + r_0 + sh_0, \tag{5}$$

where r_n are the residues, p_n are the poles, r_0 is a constant term, and h_0 is a proportional part.

When smooth frequency responses are considered, such as the series impedance $\check{Z}(s_k)$ of a TL, the use of VF leads to a rational approximation with guaranteed stable poles; however, it may yield some complex conjugate poles and residues.

VF-RP ensures a model with only real poles and residues based on the non-dominance property of the complex poles in smooth function approximations. In VF-RP, each complex pair of poles is replaced with two real poles separated by a distance δ:

$$s - (\gamma_n \pm j\beta_n) \rightarrow [s - (\omega_n + \delta)], [s - (\omega_n - \delta)]. \tag{6}$$

With ${\omega_n}^2 = {\gamma_n}^2 + {\beta_n}^2$ and $\delta = 0.01$, as recommended in [8]. Fig. 2 illustrates how even three or four poles could be considered in the replacement to avoid the possible increase in RMS error. The rationale for using this pole replacement strategy is that complex poles should not be dominant, and when they are, their behavior more closely resembles a repeated pair of real poles [8].

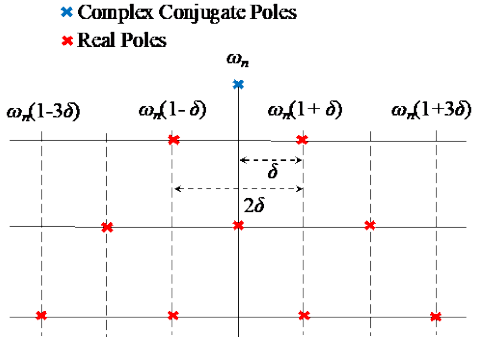

Fig. 2. Complex conjugate poles replaced by two, three, or four real poles.

B. Taku Noda's method (TN)

Based on a common ratio factor, α, this algorithm can calculate the pole position along the negative real axis of the complex plane in three different ways: A distribution with poles towards low frequencies with $\alpha > 1$, a distribution with poles towards high frequencies with $\alpha < 1$, and an equidistant distribution with $\alpha = 1$.

The method can be described as follows. First, the logarithmic frequency range of interest is defined by the first and last frequency sample as,

$$\varphi_1 = log_{10}(f_1) \text{ and } \varphi_K = log_{10}(f_K). \tag{7}$$

With $k = 1, 2, \ldots, K$. Next, considering N as the number of poles for the rational approximation and starting from the position of the first pole φ_1, the distance between φ_1 and the next pole, $\Delta\varphi_1$, is obtained by,

$$\text{if } \alpha = 1,\ \Delta\varphi_1 = \frac{\varphi_K - \varphi_1}{N},$$
$$\text{if } \alpha \neq 1,\ \Delta\varphi_1 = (\varphi_K - \varphi_1)\left(\frac{1-\alpha}{1-\alpha^{N-1}}\right). \tag{8}$$

The following distances between poles are then calculated using,

$$\Delta\varphi_n = \Delta\varphi_1 \alpha^{n-1},\ n = 1, 2, \dots, N. \tag{9}$$

According to the intervals obtained, the position of the poles in logarithmic frequency are,

$$\varphi_n = \varphi_1 + \sum_{n=1}^{n-1} \Delta\varphi_1 \alpha^{n-1}. \tag{10}$$

Finally, the *n*th pole is given by,

$$P_n = -2\pi 10^{\varphi_n}. \tag{11}$$

In this work, the equidistant distribution with $\alpha = 1$ is used, as recommended by the author in [9].

C. Residue identification

After pole identification, using either the VF-RP or TN method, the residues for the rational approximation (5) must be calculated by solving (5) as a Least Squares (LS) problem, $\mathbf{Ax} \cong \mathbf{b}$, as follows:

$$\begin{bmatrix} \frac{1}{s_1 - p_1} & \cdots & \frac{1}{s_1 - p_N} & 1 & s \\ \vdots & \ddots & \vdots & \vdots & \vdots \\ \frac{1}{s_k - p_1} & \cdots & \frac{1}{s_k - p_N} & 1 & s \end{bmatrix} \begin{bmatrix} c_1 \\ \vdots \\ c_N \\ d \\ e \end{bmatrix} \cong \begin{bmatrix} F(s_1) \\ \vdots \\ F(s_K) \end{bmatrix}. \tag{12}$$

This system can be formulated into real quantities as,

$$\begin{bmatrix} \mathrm{Re}(\mathbf{A}) \\ \mathrm{Im}(\mathbf{A}) \end{bmatrix} \mathbf{x} \cong \begin{bmatrix} \mathrm{Re}(\mathbf{b}) \\ \mathrm{Im}(\mathbf{b}) \end{bmatrix}. \tag{13}$$

Given an overdetermined system, $\widetilde{\mathbf{A}}\mathbf{x} \cong \tilde{\mathbf{b}}$, where the objective function to be minimized is,

$$\min_{\mathbf{x}} \left\| \widetilde{\mathbf{A}}\mathbf{x} - \tilde{\mathbf{b}} \right\|_2. \tag{14}$$

The system's solution satisfies the normal equations,

$$\widetilde{\mathbf{A}}^{\mathrm{t}} \widetilde{\mathbf{A}}\mathbf{x} \cong \widetilde{\mathbf{A}}^{\mathrm{t}} \tilde{\mathbf{b}}. \tag{15}$$

Finally, the unconstrained LS solution is,

$$\mathbf{x} \cong \left(\widetilde{\mathbf{A}}^{\mathrm{t}} \widetilde{\mathbf{A}}\right)^{-1} \widetilde{\mathbf{A}}^{\mathrm{t}} \tilde{\mathbf{b}}. \tag{16}$$

In the numerical implementation, column scaling is commonly used [1-3], with techniques such as QR decomposition [1-3] or SVD [9] also being proposed.

IV. Residue identification via NNLS

Given the constraints imposed on the impedance model $Z(s; \mathbf{x})$ in Section II, a Constrained LS problem is formulated in which the residues must be positives. The problem to be solved for calculating the residues thus becomes,

$$\min_{\mathbf{x}} \left\| \widetilde{\mathbf{A}}\mathbf{x} - \tilde{\mathbf{b}} \right\|_2 \text{ subject to } \mathbf{x} \geq \mathbf{0}. \tag{17}$$

This is a Non-negative Least Squares problem (NNLS) [18]. The algorithm implemented to solve this problem is described in [18-19] and presented in Table I, where the algorithm steps are divided into sections A, B, and C. The NNLS algorithm is available in MATLAB as *lsqnonneg*.

Assuming a proper function in (5), there are N inequality constraints according to (17). The *n*th constraint is active if the *n*th solution is negative or zero if solved by (16); otherwise, the constraint is considered non-active.

NNLS is an active set algorithm based on the premise that, given a known active set Q (A.1), the solution to the LS problem is reduced to solving an unconstrained LS problem involving only the non-active variables, P (A.2). The variables in the active set are constrained to zero. To find the solution, a stepwise manner LS algorithm is applied, beginning with a vector that satisfies the constraints (A.3). Based on the calculation of a gradient vector (A.4), the variables are identified in each step of the algorithm and moved from the active set Q to the non-active set P.

After a finite number of iterations [18], the complete active set is found, and the solution is calculated by solving the LS problem of the unconstrained subset of variables. The optimal solution has been found when,

$$w_m = 0,\ m \in P \text{ and } w_m < 0,\ m \in Q \tag{18}$$

V. Test cases

In this section, two overhead line configurations are used to test the proposed methodology:

1) Single-phase transmission line.
2) Three-phase double-circuit horizontal transmission line.

TABLE I
NON-NEGATIVE LEAST SQUARES ALGORITHM

Input: $\widetilde{\mathbf{A}} \in \mathbb{R}^{2K \times N}$ and $\tilde{\mathbf{b}} \in \mathbb{R}^{2K}$
Output: $\mathbf{x} \in \mathbb{R}^N$ subject to $\mathbf{x} \geq \mathbf{0}$

A. *Initialization*
- A.1: $Q = \{1, 2, \dots, N\}$
- A.2: $P = \varnothing$
- A.3: $\mathbf{x} = 0$
- A.4: $\mathbf{w} = \widetilde{\mathbf{A}}^{\mathrm{t}}(\tilde{\mathbf{b}} - \widetilde{\mathbf{A}}\mathbf{x})$

B. *Main loop*
- B.1: Proceed if $Q \neq \varnothing \wedge \left[\max_{n \in Q}(w_n) > tolerance\right]$
- B.2: $m = \max_{n \in Q}(w_n)$
- B.3: Include the index m in P and remove it from Q
- B.4: $\mathbf{s}^P \cong \left[(\widetilde{\mathbf{A}}^P)^{\mathrm{t}} \widetilde{\mathbf{A}}^P\right]^{-1} (\widetilde{\mathbf{A}}^P)^{\mathrm{t}} \tilde{\mathbf{b}}$

C. *Inner loop*
- C.1: Proceed if $\min(\mathbf{s}^P) \leq 0$
- C.2: $\alpha = -\min_{n \in P}[x_n / (x_n - s_n)]$
- C.3: $\mathbf{x} := \mathbf{x} + \alpha(\mathbf{s} - \mathbf{x})$
- C.4: Update Q and P
- C.5: $\mathbf{s}^P \cong \left[(\widetilde{\mathbf{A}}^P)^{\mathrm{t}} \widetilde{\mathbf{A}}^P\right]^{-1} (\widetilde{\mathbf{A}}^P)^{\mathrm{t}} \tilde{\mathbf{b}}$
- C.6: $\mathbf{s}^Q = 0$

End C
- B.5: $\mathbf{x} = \mathbf{s}$
- B.6: $\mathbf{w} = \widetilde{\mathbf{A}}^{\mathrm{t}}(\tilde{\mathbf{b}} - \widetilde{\mathbf{A}}\mathbf{x})$

End B

A. Single-phase transmission line.

The line configuration is shown in Fig. 3a. This example was presented in [7] together with the methodology presented in Section II; where some elements such as negative resistances and inductances were reported.

The behavior of the series impedance $(\check{Z}_k)$ with $K = 500$ samples is shown in Fig. 3b, and Fig. 4a shows the rational approximation results for $\hat{Z}_k$ (3) using the TN and VF-RP methods with $N = 30$ poles. It can be observed that $\hat{Z}_k$ has a smoother behavior than $\check{Z}_k$, whose rational approximation results, shown in Fig. 4b, demonstrate that the fitting deviation calculated using the absolute error is better with VF-RP.

The zero-pole diagram for the rational approximations of $\hat{Z}_k$ using TN and VF-RP are shown in Figs. 5a and 5b, respectively. In this case, the VF-RP method satisfies the alternation condition in (4); the TN method does not. Fig. 6 shows the same results as Fig. 4 but using NNLS for residue calculation.

The zero-pole diagram in Fig. 7a reveals that 2 of the 30 poles have been eliminated in the TN method, that is, their residues are zero and those poles can therefore be disregarded. Despite the elimination of these poles, the precision of the fitting remains quite similar, with the advantage that positive elements are obtained for the model. In the case of VF-RP using NNLS it remains the same, as seen in Fig. 7b.

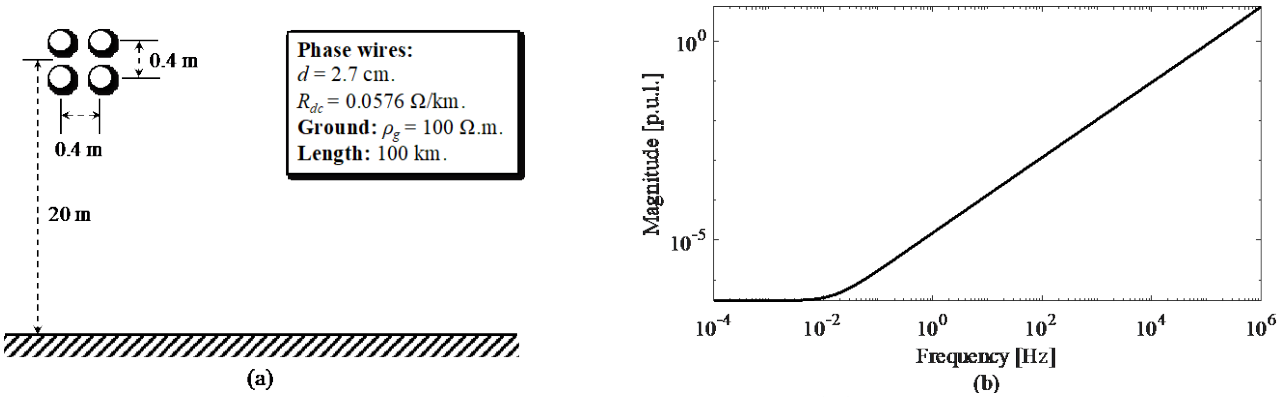

Fig. 3. (a) Single-phase transmission line configuration, (b) Behavior of the series impedance $(\check{Z}_k)$ of the single-phase transmission line.

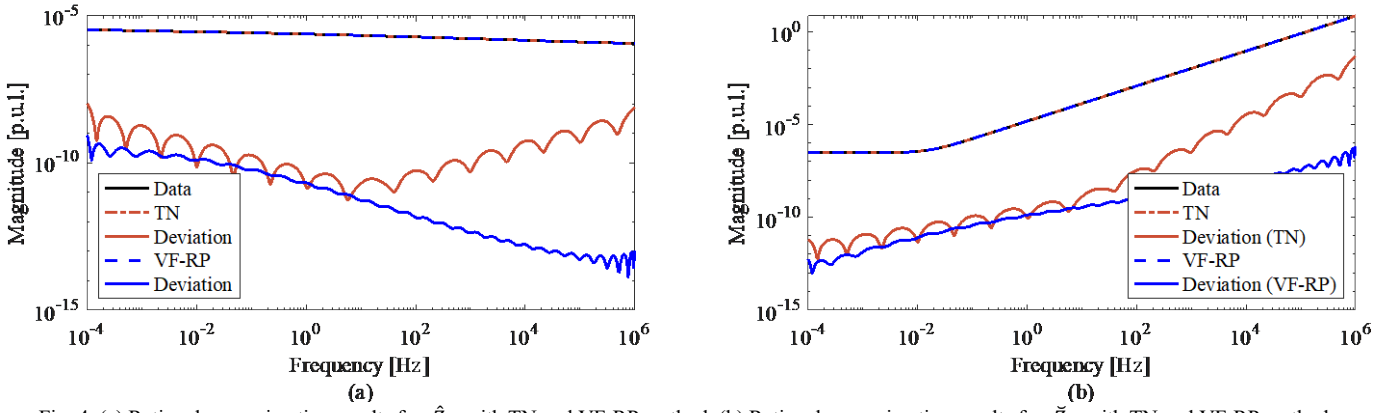

Fig. 4. (a) Rational approximation results for $\hat{Z}_k$ with TN and VF-RP method, (b) Rational approximation results for $\check{Z}_k$ with TN and VF-RP method.

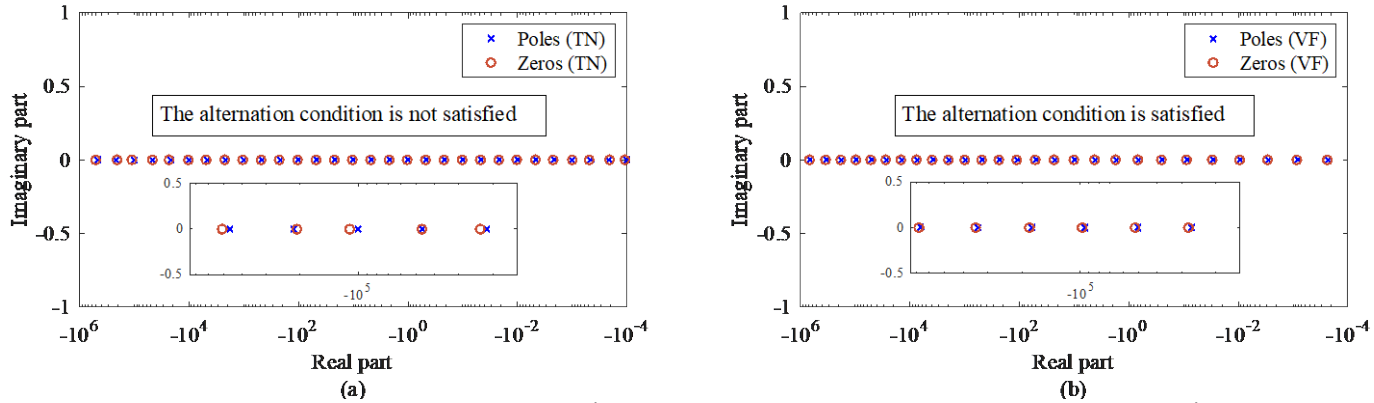

Fig. 5. (a) Zero-pole diagram for the rational approximation of $\hat{Z}_k$ with TN, (b) Zero-pole diagram for the rational approximation of $\hat{Z}_k$ with VF-RP.

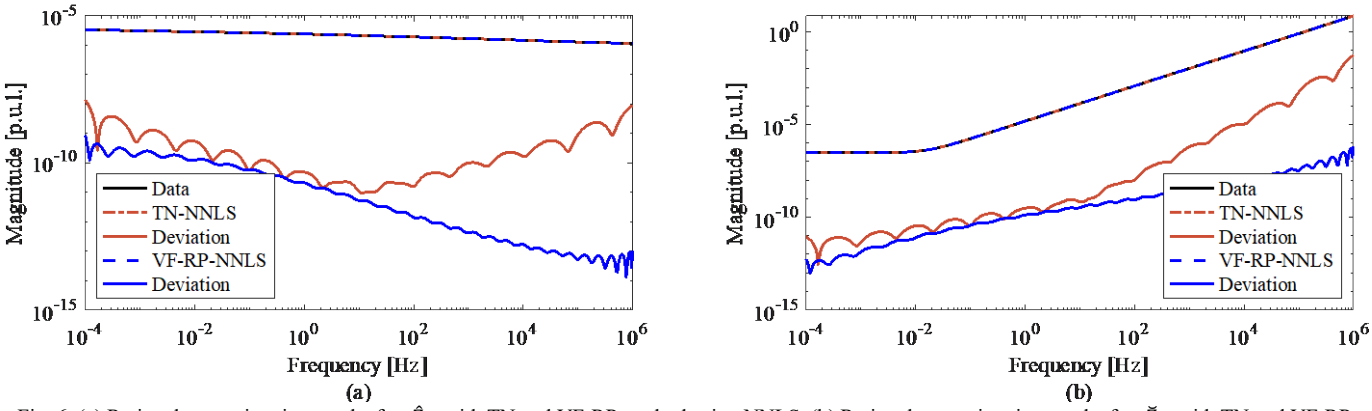

Fig. 6. (a) Rational approximation results for $\hat{Z}_k$ with TN and VF-RP method using NNLS, (b) Rational approximation results for $\check{Z}_k$ with TN and VF-RP method using NNLS.

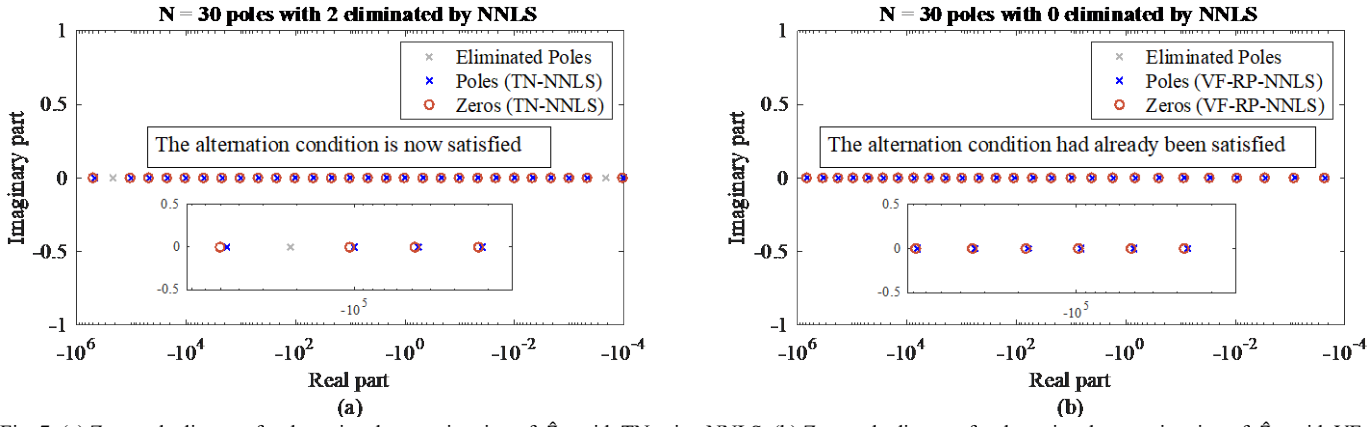

Fig. 7. (a) Zero-pole diagram for the rational approximation of $\hat{Z}_k$ with TN using NNLS, (b) Zero-pole diagram for the rational approximation of $\hat{Z}_k$ with VF-RP using NNLS.

Next, Figs. 8 and 9 show the same results but using $N = 70$ poles; residue calculation using NNLS eliminates 37 and 35 poles for TN and VF-RP, respectively. This indicates that the rational approximation should be carried out using approximately 35 poles. This approach ensures that all the elements of the model $Z(s;\mathbf{x})$ in (2) are positive, thereby guaranteeing model passivity. The zero-pole diagram for TN method and VF-RP are shown in Fig. 9a and 9b, respectively. Fig. 9b also shows the poles to which the conventional VF algorithm converges, with some real and others complex. Based on this result, VF-RP is applied where each pair of complex conjugate poles is replaced by two real poles.

Finally, the energization of open-circuited line is tested using the ATPDraw and ATP-EMTP. The line is energized from a 1 p.u. voltage source behind an impedance of $R_s = 0.5\ \Omega$ and $L_s = 0.03$ H and with $\Delta t = 0.5\ \mu$s.

Fig. 10 presents the voltage at the receiving end using: 1) The JMarti-ATP model, 2) a cascade of 10 π-circuits with 33 branches for TN-NNLS, and 3) a cascade of 10 π-circuits with 35 branches for VF-RP-NNLS.

These results show that simulations using the cascades of π-circuits are very accurate and they are carried out using only positive R, L, and C elements.

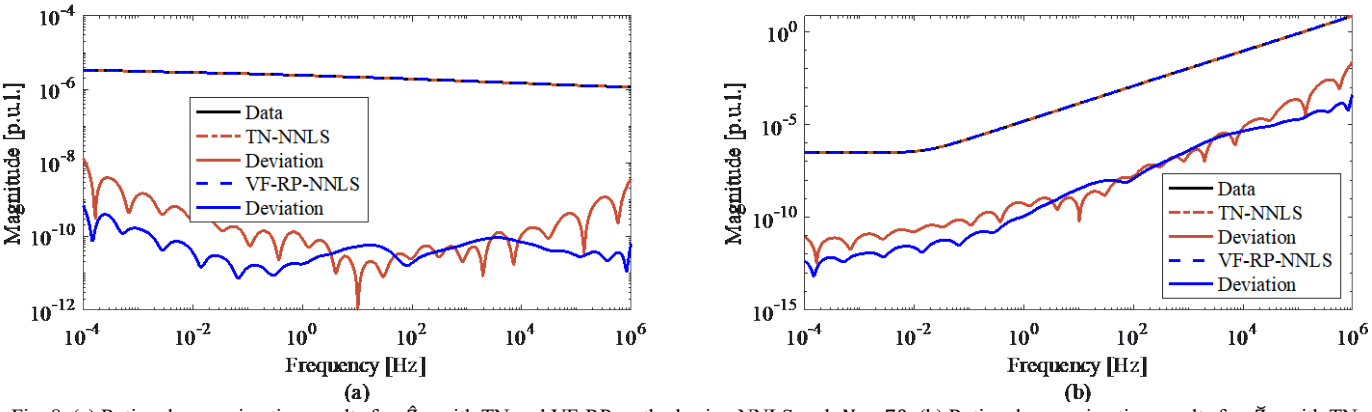

Fig. 8. (a) Rational approximation results for $\hat{Z}_k$ with TN and VF-RP method using NNLS and $N = 70$, (b) Rational approximation results for $\check{Z}_k$ with TN and VF-RP method using NNLS and $N = 70$.

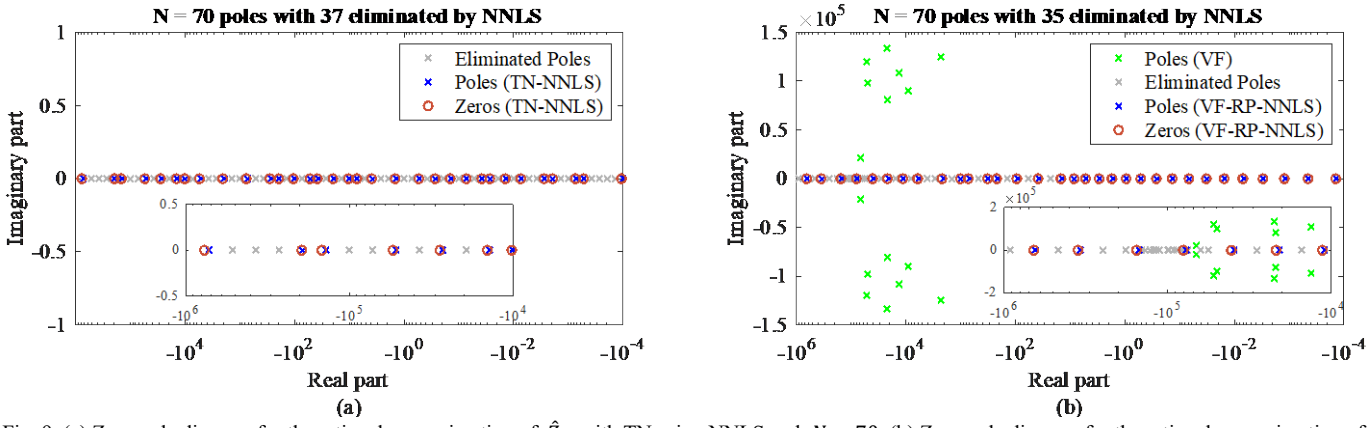

Fig. 9. (a) Zero-pole diagram for the rational approximation of $\hat{Z}_k$ with TN using NNLS and $N = 70$, (b) Zero-pole diagram for the rational approximation of $\hat{Z}_k$ with VF-RP using NNLS and $N = 70$.

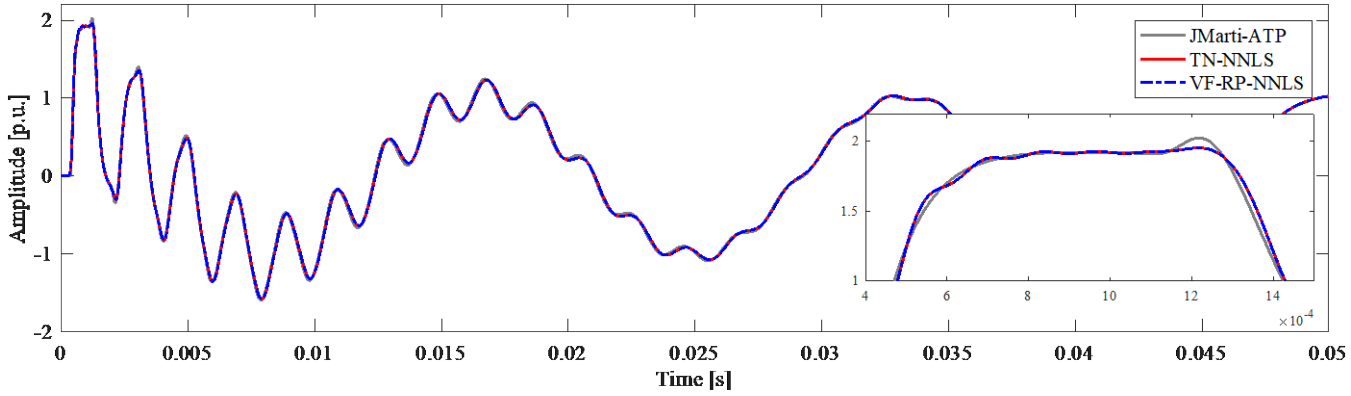

Fig. 10. Voltage at receiving end for the single-phase transmission line configuration using: 1) The JMarti-ATP model, 2) a cascade of 10 π-circuits with 33 branches for TN-NNLS and 3) a cascade of 10 π-circuits with 35 branches for VF-RP-NNLS.

B. Three-phase double-circuit horizontal transmission line.

The line configuration is shown in Fig. 11a. This example was presented in [8] together with the VF-RP methodology to improve the computational efficiency of the Universal Line Model.

The behavior of the series impedance matrix $(\breve{\mathbf{Z}}_k)$ with $K = 500$ samples is shown in Fig. 11b and in Fig. 12a the corresponding for $\hat{\mathbf{Z}}_k$. In Fig. 12b is shown the trace fitting of $\hat{\mathbf{Z}}_k$ with TN and VF-RP method using NNLS and $N = 50$.

This enables the use of common poles [20] for each matrix element. The trace of $\hat{\mathbf{Z}}_k$ clearly exhibits smooth behavior, and the fitting deviation calculated using absolute error is lower with VF-RP.

Figure 13a and 13b depict the zero-pole diagrams for the rational approximations of the trace of $\hat{\mathbf{Z}}_k$ using TN, VF-RP, and NNLS.

Both TN method and VF-RP methods satisfy the alternation condition established in (4). Residue calculation using NNLS eliminates 19 poles for the TN method and 14 for the VF-RP method.

Finally, Figs. 14a and 14b show the rational approximation results for the TN and VF-RP methods using NNLS and common poles for $\hat{\mathbf{Z}}_k$ and $\breve{\mathbf{Z}}_k$, respectively.

After pole identification based on the trace, each set of residues must be calculated for each element of the matrix $\hat{\mathbf{Z}}_k$. NNLS is employed once more, and some residues may be eliminated due to their zero values, leading to the removal of corresponding poles.

Finally, Table II and Table III list the number of removed poles for each element of the matrix $(\hat{\mathbf{Z}}_k)$ of the 31 and 36 that remained in the case of TN and VF-RP methods, respectively.

TABLE II
NUMBER OF REMOVED POLES FOR EACH ELEMENT OF THE MATRIX $(\hat{\mathbf{Z}}_k)$ FOR TN-NNLS

2	3	3	3	3	3
3	2	3	3	3	3
3	3	2	3	3	3
3	3	3	2	3	3
3	3	3	3	2	3
3	3	3	3	3	2

TABLE III
NUMBER OF REMOVED POLES FOR EACH ELEMENT OF THE MATRIX $(\hat{\mathbf{Z}}_k)$ FOR VF-RP-NNLS

1	0	1	1	1	1
0	1	0	2	1	1
1	0	1	1	2	2
1	2	1	1	1	0
1	1	2	1	1	1
1	1	2	0	1	1

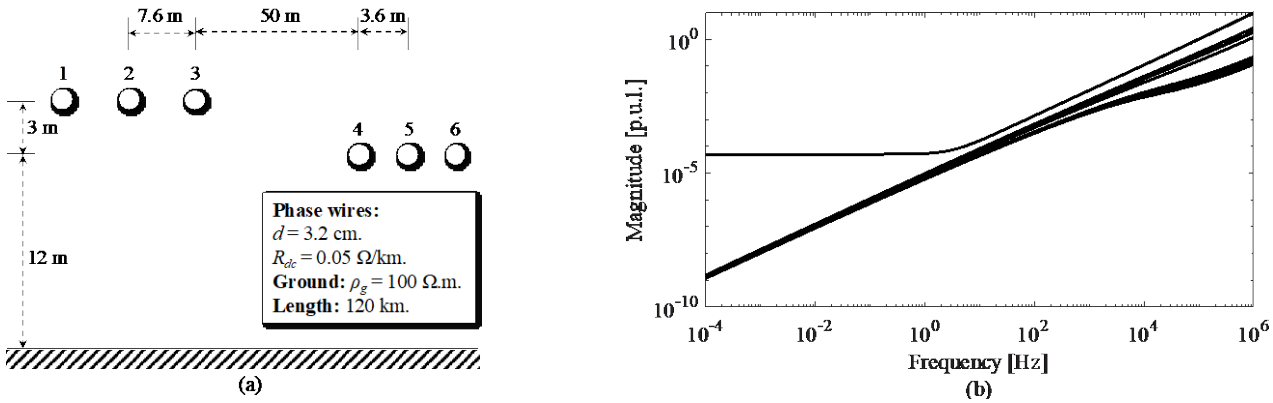

Fig. 11. (a) Three-phase double-circuit horizontal transmission line configuration, (b) Behavior of the series impedance matrix for $\breve{\mathbf{Z}}_k$.

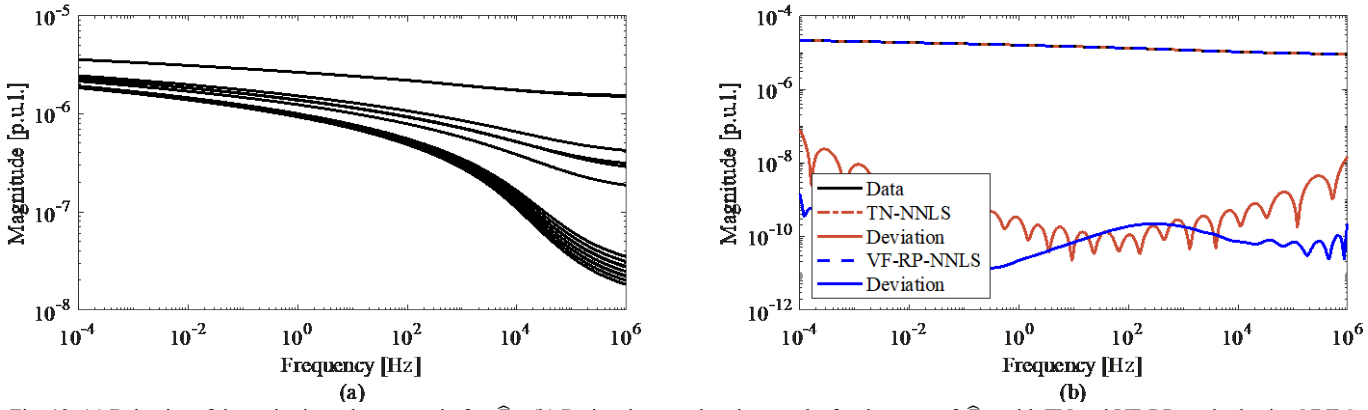

Fig. 12. (a) Behavior of the series impedance matrix for $\hat{\mathbf{Z}}_k$, (b) Rational approximation results for the trace of $\hat{\mathbf{Z}}_k$ with TN and VF-RP method using NNLS and with $N = 50$.

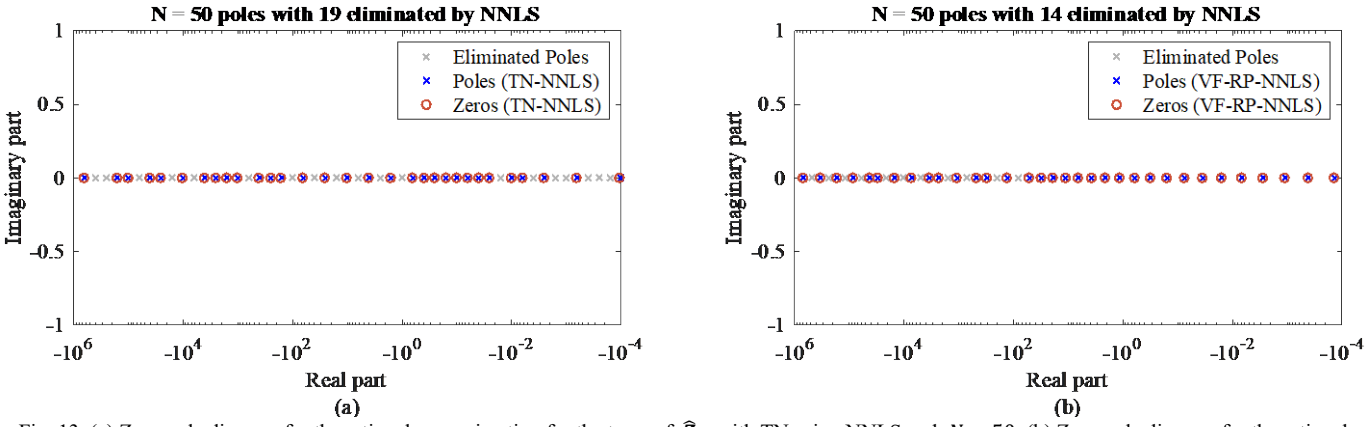

Fig. 13. (a) Zero-pole diagram for the rational approximation for the trace of $\hat{\mathbf{Z}}_k$ with TN using NNLS and $N = 50$, (b) Zero-pole diagram for the rational approximation for the trace of $\hat{\mathbf{Z}}_k$ with VF-RP using NNLS and with $N = 50$.

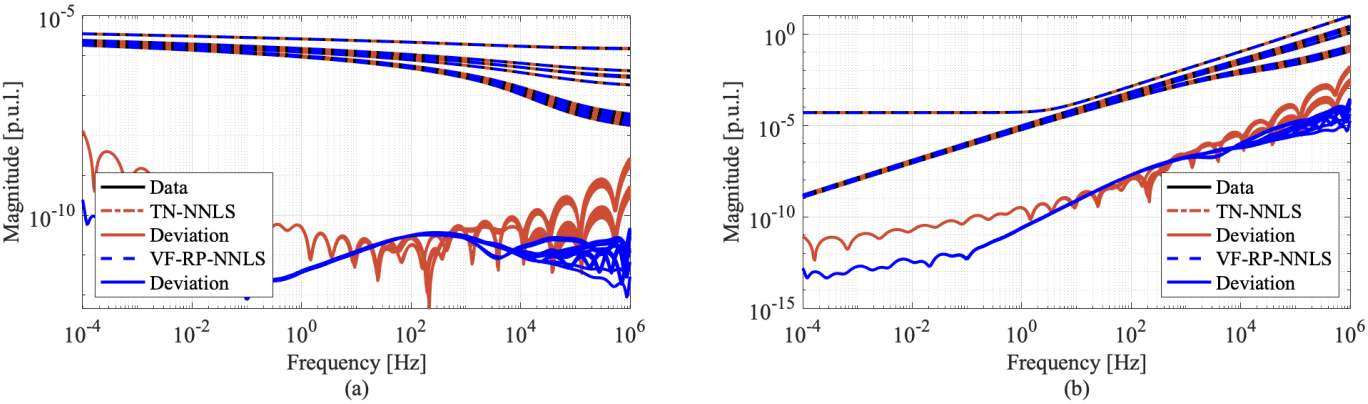

Fig. 14. (a) Rational approximation results for $\hat{\mathbf{Z}}_k$ with TN and VF-RP method using NNLS and common poles, (b) rational approximation results for $\breve{\mathbf{Z}}_k$ with TN and VF-RP method using NNLS and common poles.

VI. Discussion

The presented methodology for obtaining a passive model of the transmission line impedance $(\check{Z}_k)$ is based on a correct problem statement, which means, the correct use of the rational fitting techniques. Please consider that the series impedance can be approximated as

$$\check{Z}_k \cong \sum_{n=1}^{N} \frac{sR'_n}{s + (R'_n/L'_n)} + R'_0 + sL'_0. \tag{19}$$

It is possible to modify (19) to

$$\check{Z}_k \cong \sum_{n=1}^{N} \frac{-\left(\frac{R'^{\,2}_n}{L'_n}\right)}{s + (R'_n/L'_n)} + (R'_0 + R'_1 + R'_2 \dots R'_N) + sL'_0. \tag{20}$$

Please note that VF (5) can be directly used to carry out the rational approximation of $\check{Z}_k$ given the model in (20) where the residues must be negative.

Instead, (19) can easily be modified to

$$\hat{Z}_k = \frac{\check{Z}_k}{s} \cong \sum_{n=1}^{N} \frac{R'_n}{s + (R'_n/L'_n)} + \frac{R'_0}{s} + L'_0. \tag{21}$$

Although the second term on the right in (21) is not considered in VF, since it is a known parameter (21) can be modified to

$$\hat{Z}_k = \frac{\check{Z}_k - R'_0}{s} \cong \sum_{n=1}^{N} \frac{R'_n}{s + (R'_n/L'_n)} + L'_0. \tag{22}$$

In this case, division by s also allows obtaining a function with smooth behavior $(\hat{Z}_k)$ and being fitted with real poles and implementing NNLS to calculate positive residues.

VII. Conclusions

This paper presented the implementation of the NNLS method to synthesize a rational function-based model with positive parameters (resistors, inductances, and capacitances) and thus guarantee its passivity. The main findings are:

1) Both the VF-RP and TN methods achieve acceptable fitting deviations for the series impedance approximation of a TL using real poles. However, they do not guarantee that residue calculations are positive, nor do they guarantee positive elements as a result.
2) The fitting deviations for the rational approximations presented using VF-RP were better than those obtained using the TN method.
3) The NNLS method can be used in both VF-RP and TN fitting techniques.
4) In the case of the TN method, more pole-residue pairs are eliminated compared to VF-RP when NNLS is implemented to obtain positive residues.
5) In matrix fitting, the trace concept can be also used to obtain common poles for the rational approximation using this methodology.

VIII. References

[1] E.S. Bañuelos-Cabral, J.A. Gutiérrez-Robles, B. Gustavsen, J.L. Naredo, J.L. García-Sánchez, J. Sotelo-Castañón, V.A. Galván-Sánchez, "Enhancing the accuracy of rational function-based models using optimization," *Electric Power Systems Research,* vol. 125, pp. 83-93, April 2015.

[2] S. Grivet-Talocia and B. Gustavsen, *Passive Macromodeling. Theory and applications*, John Wiley & Sons, Inc., 978-1118094914, 2015.

[3] E.S. Bañuelos-Cabral, J.A. Gutiérrez-Robles and B. Gustavsen, *Rational Fitting Techniques for the Modeling of Electric Power Components and Systems Using MATLAB Environment*, Intechopen, 978-953-51-3674-3, 2017.

[4] B. Gustavsen, "Passivity Enforcement by Residue Perturbation via Constrained Non-Negative Least Squares," *IEEE Transactions on Power Delivery*, vol. 36, no. 5, pp. 2758-2767, Oct. 2021.

[5] M. S. Sarto, A. Scarlatti and C. L. Holloway, "On the use of fitting models for the time-domain analysis of problems with frequency-dependent parameters," *2001 IEEE EMC International Symposium. Symposium Record. International Symposium on Electromagnetic Compatibility*, vol.1, pp. 588-593, Montreal, QC, Canada, 2001.

[6] Sérgio Kurokawa, Fábio N.R. Yamanaka, Afonso J. Prado, José Pissolato, "Inclusion of the frequency effect in the lumped parameters transmission line model: State space formulation," *Electric Power Systems Research*, vol. 79, no. 7, pp. 1155-1163, February 2009.

[7] Tainá F.G. Pascoalato, Anderson R.J. de Araújo, Sérgio Kurokawa, José Pissolato Filho, "Alternative method to include the frequency-effect on transmission line parameters via state-space representation," *International Journal of Electrical Power & Energy Systems*, vol. 155, July 2024.

[8] E.S. Bañuelos-Cabral, B. Gustavsen, J.A. Gutiérrez-Robles, et al. "Computational efficiency improvement of the Universal Line Model by use of rational approximations with real poles," *Electric Power Systems Research*, vol. 140, pp. 424-434, May 2016.

[9] T. Noda, "Synthesis of a Transfer Function with Real Poles from Tabulated Frequency Response Data for Transmission-Line Impedance Modeling," *IEEE Access*, vol. 10, pp. 86029-86037, 2022.

[10] B. Gustavsen and A. Semlyen, "Rational approximation of frequency domain responses by vector fitting," *IEEE Transactions on Power Delivery*, vol. 14, no. 3, pp. 1052-1061, July 1999,

[11] Bañuelos-Cabral, E.S., Gutiérrez-Robles, J.A., García-Sánchez, J.L. et al. "Accuracy enhancement of the JMarti model by using real poles through vector fitting," *Electrical Engineering*, vol. 101, pp. 635–646, July 2019.

[12] J. S. L. Colqui, L. C. T. Eraso, P. T. Caballero, J. P. Filho and S. Kurokawa, "Implementation of Modal Domain Transmission Line Models in the ATP Software," *IEEE Access*, vol. 10, pp. 15924-15934, January 2022.

[13] J. S. L. Colqui, A. R. J. D. Araújo, T. F. G. Pascoalato, S. Kurokawa and J. P. Filho, "Transient Analysis on Multiphase Transmission Line Above Lossy Ground Combining Vector Fitting Technique in ATP Tool," *IEEE Access*, vol. 10, pp. 86204-86214, August 2022.

[14] P. Juan Robles Balestero, J. S. L. Colqui and S. Kurokawa, "Using the Exact Equivalent π-Circuit of Transmission Lines for Electromagnetic Transient Simulations in the Time Domain," *IEEE Access*, vol. 10, pp. 90847-90856, August 2022.

[15] Robles Balestero, Juan Paulo, Jaimis Sajid Leon Colqui, and Sérgio Kurokawa, "Using the Exact Equivalent π-Circuit Model for Representing Three-Phase Transmission Lines Directly in the Time Domain," *Energies*, vol. 16, no. 20, October 2023.

[16] Thomas Treider, Hans Kristian Høidalen, "Estimating distance to transient and restriking earth faults in high-impedance grounded, ring-operated distribution networks using current ratios," *Electric Power Systems Research*, vol. 224, August 2023.

[17] Omar Wing, *Classical Circuit Theory*, Springer, 2008, 978-0-387-09739-8.

[18] Charles L. Lawson and Richard J. Hanson, *Solving Least Squares Problems*, Society for Industrial and Applied Mathematics, 1995, 978-0898713565, 2015.

[19] R. Bro, S. De Jong, "A fast Non-negativity-constrained Least Squares Algorithm," *Journal of Chemometric*, vol. 11, pp. 393-401, 1997.

[20] B. Gustavsen and J. Nordstrom, "Pole Identification for The Universal Line Model Based on Trace Fitting," *IEEE Transactions on Power Delivery,* vol. 23, no. 1, pp. 472-479, Jan. 2008.*ff*